Citation:
Emami, H, Sarkhosh, N, Bui, L and Mitchell, A 2008, 'Amplitude independent RF instantaneous frequency measurement system using photonic Hilbert transform', Optics Express, vol. 16, no. 18, pp. 13707-13710.

Amplitude independent RF instantaneous frequency measurement system using photonic Hilbert transform

H. Emami*, N. Sarkhosh, L. A. Bui, and A. Mitchell

Microelectronics and Material Technology Center
School of Electrical and Computer Engineering
Royal Melbourne Institute of Technology
GPO Box 2476V, Melbourne, Victoria, 3001, Australia
Corresponding author: hossein.emami@rmit.edu.au

Abstract: A photonic instantaneous frequency measurement system capable of measuring both RF frequency and power simultaneously, is conceived and practically demonstrated. This system employs an RF photonic Hilbert transformer together with low-cost, low-frequency photo-detectors to obtain two orthogonal DC measurements. This system exhibits a frequency range of 1-10 GHz. Wider frequency range can be achieved through integration.

OCIS codes: (0060.5625) Radio frequency photonics; (060.2360) Fiber optics links and subsystems; (070.6020) Continuous optical signal processing; (350.4010) Microwaves.

References and links

1. H. Gruchala and M. Czyzewski, "The instantaneous frequency measurement receiver in the complex electromagnetic environment," in *Proceedings of International Conference on Microwave, RADAR, and Wireless Communications (MIKON2004)* **1**, 155-158 (2004).
2. J. B. Y. Tsui and D. L. Sharpin, "Frequency measurement receiver with bandwidth improvement through synchronized phase shifted sampling," United States Patent 5198746, 30 Mar. 1993.
3. L. Fan, C-H. Ho, S. Lanamaluru, and K. Chang, "Wide-band reduced-size uniplanar magic-T, hybrid-ring, and de Ronde's CPW-slot couplers," IEEE Trans. Microwave Theory Tech. **43**, 2749-2758 (1995).
4. S. Kumar, A. Mohammadi, and D. Klymyshyn, "A direct 64QAM modulator suitable for MMIC applications," Microwave J. **40**, 116-122 (1997).
5. L. V. T. Nguyen and D. B. Hunter, "A photonic technique for microwave frequency measurement," IEEE Photon. Technol. Lett. **18**, 1188-1190 (2006).
6. A. J. Seeds and K. J. Williams, "Microwave photonics," IEEE J. Lightwave Technol. **24**, 4628-4641 (2006).
7. R. A. Minasian, "Photonic signal processing of microwave signals," IEEE Trans. Microwave Theory Technol. **54**, 832-846 (2006).
8. J. Capmany, B. Ortega, and D. Pastor, "A tutorial on microwave photonic filters," J. Lightwave Technol. **24**, 201-229 (2006).
9. H. Emami, N. Sarkhosh, L. A. Bui, and A. Mitchell, "Wideband RF photonic in-phase and quadrature-phase generation," Opt. Lett. **33**, 98-100 (2008).
10. N. Sarkhosh, H. Emami, L. A. Bui, and A. Mitchell, "Reduced cost microwave photonic instantaneous frequency measurement system," IEEE Photon. Technol. Lett. *In Press*

1. Introduction

Instantaneous Frequency Measurement (IFM) receivers are an important part of RADAR warning receivers. These receivers provide efficient real time frequency identification of unknown thread signals. Traditional IFM receivers, have been implemented using microwave interferometers incorporated from wide band quadrature hybrid couplers and delay lines [1, 2]. Im-

#95839 - $15.00 USD Received 15 May 2008; revised 14 Aug 2008; accepted 19 Aug 2008; published 21 Aug 2008

plementing wide band hybrid couplers can be challenging due to unavoidable radiation and dispersion in microwave domain [3, 4].

In the recent years, microwave-photonics has been introduced as a means of increasing the bandwidth of microwave signal processing systems [5-10]. Therefore it has been investigated for IFM implementation [5].

In order to independently measure frequency and amplitude, orthogonal measurement of the signal must be made [1, 2]. Traditionally, this is achieved using hybrid couplers in the microwave domain to obtain in-phase and quadrature-phase interferometry. Recently we have demonstrated a technique to achieve in-phase and quadrature-phase shifting in the optical domain using photonic transversal filter [9].

Recent investigation has used broad band photo-detectors to obtain IFM measurements [5]. Implementing banks of these devices would thus be expensive. Another photonic implementation has been demonstrated based on DC component present at the output of inexpensive low-frequency photo-detectors [10]. This implementation is limited as the RF power must be known to identify the RF frequency unambiguously .

In this paper, we proposed an IFM system capable of measuring both RF frequency and power independently. This system employs a transversal approach to implement a Hilbert transformer which provides two orthogonal DC measurements to perform simultaneous frequency and power measurement. We have succeeded in achieving frequency measurement from 1-10 GHz using only DC photo-detection.

2. Orthogonal measurement IFM concept

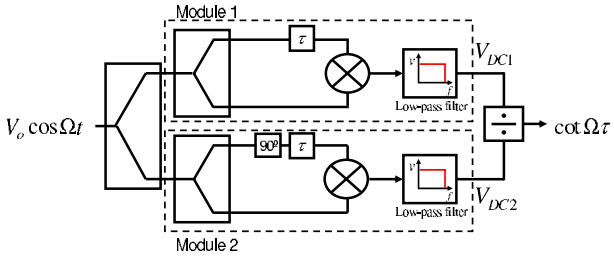

Fig. 1. Block diagram of an IFM system .

Several IFM systems have been reported [1, 2]. One possibility is presented in Fig. 1. A single RF tone is divided into two equal portions feeding two modules; Module 1, and Module 2, within each module, the RF tone is further divided into two equal portions. One portion is delayed relative to the other by time τ. The two portions are then multiplied together and the output is DC-filtered. The DC output of each module is a sinusoidal function of frequency. A 90° phase shift is introduced in one arm of Module 2 causes its output to have a sin response while Module 1 has a cosine response. It can be easily shown that if the RF tone is defined as $V_\circ cos\Omega t$, the DC voltages, present at the output of the Low-pass filters, are:

$$V_{DC1} = \frac{1}{8}V_\circ^2 cos\Omega\tau \quad , \quad V_{DC2} = \frac{1}{8}V_\circ^2 sin\Omega\tau \tag{1}$$

The ratio of these voltages is $cot\Omega\tau$, which is a function of RF frequency but is independent of the RF tone amplitude ($V_\circ$). This establishes an amplitude ($V_\circ$) independent relation between the IFM output signal and the input RF frequency. Once we have established the measured frequency, the amplitude can also be measured using the output of either Module 1 or Module 2 using V_{DC1} or V_{DC2} equation, respectively. As the output signals are DC terms, this system

#95839 - $15.00 USD Received 15 May 2008; revised 14 Aug 2008; accepted 19 Aug 2008; published 21 Aug 2008

can be implemented low-cost while still enabling broad band frequency measurement; however, practical implementation of such system, requires broad band delays and mixers which can be challenging in the microwave domain. Microwave photonics may thus be an attractive solution.

3. Orthogonal measurement IFM system proposal

In this section we introduce a photonic approach that can be employed to implement the IFM system of Section 2. As the system exhibits a frequency dependent DC output, low-cost photo-detectors can be used to reduce the total cost of the system. Also by using photonic elements, a broad frequency detection range can be achieved. To achieve the broad band 90 ° phase shift required in Fig. 1, a Hilbert transformer [9] can be employed in which, a two-tap transversal filter with an additional reference tap is used to make orthogonal measurements. This gives a broad band 90° phase shift; however as there are nulls in the transversal response, the frequency measurement range will be limited between two null frequencies.

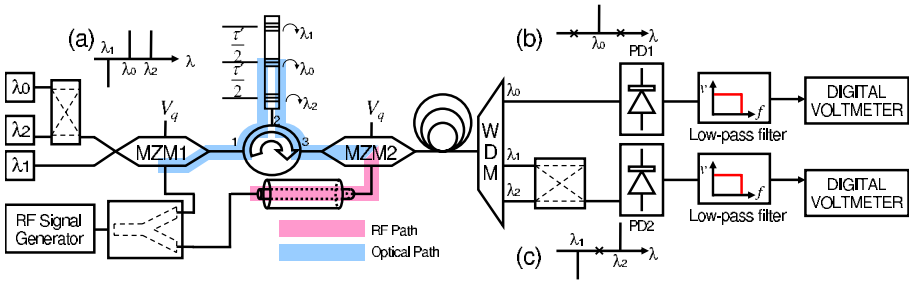

Fig. 2. Experimental set-up of IFM system with orthogonal outputs.

Figure 2 shows the experimental set-up of the photonic IFM with orthogonal outputs. An RF signal generator produces a single RF tone divided into two equal portions feeding two arms of the IFM system. These arms are labelled the Optical Path and the RF Path on Fig. 2. The RF tone in the Optical Path, modulates three wavelengths being used to implement a two-tap (λ_1, and λ_2) transversal filter with a reference tap ($\lambda_\circ$) in between. Carriers $\lambda_\circ$ and λ_2 are combined using a 3dB optical coupler. This combined signal together with λ_1 are modulated oppositely to make the desired combination as shown in Fig. 2 inset a) [9]. The modulated signal is then input to Port 1 of an optical circulator. Port 2 of the circulator is connected to a cascaded grating. Each wavelength is reflected with different but uniformly incremented delays. The dispersed signal is output from Port 3 and is input to MZM2 fed with the original RF tone in the RF Path. Note the cascaded grating, and the optical circulator are both polarization maintaining. This ensures control of the polarization at the MZM2 input. The output of MZM2 is then amplified using an Erbium Doped Fiber Amplifier (EDFA) and input to a Wavelength Division Multiplexer (WDM) which separates all wavelengths. The carriers λ_1 and λ_2 are again combined using a 3dB coupler to make the two-tap transversal filter (Fig.2 inset c)) while $\lambda_\circ$ remains separated and is used as the reference (Fig. 2 inset b)). Both signals are then detected, DC-filtered and measured by digital voltmeters.

Having conceived a photonic system producing orthogonal IFM outputs, we must now develop a theoretical model predicting the behavior of the system.

4. Orthogonal measurement IFM model

To validate the ability of the experimental set-up of Fig. 2 to perform orthogonal measurements, which results in amplitude independent frequency measurement, we must develop a

#95839 - $15.00 USD Received 15 May 2008; revised 14 Aug 2008; accepted 19 Aug 2008; published 21 Aug 2008

model that predicts the frequency dependent DC output. We start with the upper photo-detector (PD1) where only wavelength $\lambda_\circ$ is present. Assuming the same V_π and loss for MZMs, the DC component of the output signal present at the output of PD1 can be described as [10]:

$$V_{DC_\circ}(\Omega) = \frac{1}{4} G Z_{PD} P_\circ \left[1 + \frac{\pi^2 (1 + M(\Omega)^2) Z_{in} P_{RF}}{4 V_\pi^2}\right] + \frac{\pi^2}{4 V_\pi^2} G M(\Omega) Z_{PD} Z_{in} P_\circ P_{RF} cos\phi(\Omega) \quad (2)$$

where $P_\circ$ is optical power corresponding to $\lambda_\circ$, V_π is the MZM half-wave voltage, P_{RF} is the RF power present at the input of each path, and Z_{PD} and Z_{in} are photo-detector output impedance and MZMs input impedance respectively. Note that MZM1 and MZM2 are assumed to have the same characteristics. The factor G can be defined as $G = r G_{LPF} L_{MZM}^2 L_{WDM} G_{EDFA}$ where r is the responsivity of the photo-detector, G_{LPF}, L_{MZM}, L_{WDM}, and G_{EDFA} are the gain of the low-pass filter, the MZMs optical insertion loss, WDM loss, and EDFA gain, respectively. The absolute magnitude response of the RF Path is $M(\Omega)$ (Fig. 2) and the phase difference of the RF Path relative to the Optical Path is $\phi(\Omega)$ (Fig. 2) [10]. For brevity, we will use M and ϕ instead of $M(\Omega)$ and $\phi(\Omega)$. Also we defined the factors $\alpha_\circ$, $\beta_\circ$, $\gamma_\circ$ as:

$$\alpha_\circ = \frac{1}{4} G Z_{PD} P_\circ, \quad \beta_\circ = \frac{1}{16} G Z_{PD} Z_{in} P_\circ \frac{\pi^2 (1 + M^2)}{V_\pi^2}, \quad \gamma_\circ = \frac{\pi^4}{2 V_\pi^2} G M Z_{PD} Z_{in} P_\circ \quad (3)$$

Eq. (2) can then be simplified as:

$$V_{DC_\circ}(\Omega) = \alpha_\circ + \beta_\circ P_{RF} + \gamma_\circ P_{RF} cos\phi \quad (4)$$

At the lower photo-detector (PD2), each wavelength (λ_1, and λ_2), generates its own DC component assuming a linear characteristic for PD2. Therefore, the DC component produced by each wavelength, present at the output of PD2 can be described as:

$$V_{DC_{\circ,1}}(\Omega) = \alpha_{90} + \beta_\circ P_{RF} - \gamma_{90} P_{RF} cos(\phi + \Omega \frac{\tau'}{2}) \quad (5)$$

$$V_{DC_{\circ,2}}(\Omega) = \alpha_{90} + \beta_\circ P_{RF} + \gamma_{90} P_{RF} cos(\phi - \Omega \frac{\tau'}{2}) \quad (6)$$

where $V_{DC_{\circ,1}}(\Omega)$, and $V_{DC_{\circ,2}}(\Omega)$ are DC components produced by wavelengths λ_1, and λ_2 respectively. The delay between λ_1 and λ_2 caused inside the cascaded grating is τ', and factors α_{90}, β_{90}, γ_{90} are defined as in Eq. (3) but with $P_\circ$ replaced by P_{90} where P_{90} is the optical power level of both carriers λ_1 and λ_2. The total DC component present at the output of PD2, can then be calculated by adding Eq. (5) and Eq. (6) and simplifying the result:

$$V_{DC_{90}}(\Omega) = 2\alpha_{90} + 2\beta_{90} P_{RF} + 2\gamma_{90} P_{RF} sin\Omega \frac{\tau'}{2} sin\phi \quad (7)$$

From Eq. (4) and Eq. (7), it can be deduced that:

$$\frac{V_{DC_\circ}(\Omega) - \alpha_\circ}{V_{DC_{90}}(\Omega) - 2\alpha_{90}} = \frac{\beta_\circ + \gamma_\circ cos\phi(\Omega)}{2\beta_{90} + 2\gamma_{90} sin\Omega \frac{\tau'}{2} sin\phi(\Omega)} \quad (8)$$

Equation (8), allows calculation of the RF frequency using the measured DC outputs without dependence on the RF power. Having RF frequency, the RF power level can also be predicted using either Eq. (4) or Eq. (7).

5. Orthogonal IFM demonstration

Having established in theory that the system of Fig. 2 should enable amplitude independent frequency measurement, we now demonstrate the IFM performance. As each parameter in Eq. (4) and Eq. (7) is known, except M and ϕ, the RF Path must first be characterized before IFM demonstration.

#95839 - $15.00 USD Received 15 May 2008; revised 14 Aug 2008; accepted 19 Aug 2008; published 21 Aug 2008

5.1. *RF Path characterization*

As Eq. (2) suggests, to predict the DC voltage of the photo-detector, it is necessary to know the absolute magnitude response of the RF Path (M) and phase response of the RF Path relative to the Optical Path (ϕ). Due to dispersive nature of the co-axial cable, the frequency dependence of M, and ϕ will be non-trivial, and therefore must be measured empirically.

The system was configured as shown in Fig. 2 whit lasers λ_1 and λ_2 were off. The laser $\lambda_\circ$ wavelength and power were set to $\lambda_0 = 1550nm$ and $P_\circ = 10.7dBm \approx 11.7mW$ respectively. A Vector Network Analyzer (VNA) was used to characterize the RF Path. To measure the phase difference ϕ of the RF Path relative to the Optical Path, Port 1 of the VNA was connected instead of RF signal generator and Port 2 of the VNA was connected to the output of the photo-detector. The VNA was then calibrated while the two ends of the co-axial cable were disconnected and replaced by two matched loads. The co-axial cable was returned while the input of MZM1 was disconnected and the Wilkinson power divider terminated with a matched load. The VNA then measured phase response of the RF Path with respect to the Optical Path. The absolute response of the RF Path (M) was also measured by the VNA with no calibration needed. Figure 3 shows the measured absolute magnitude of the RF Path (M) and phase of the

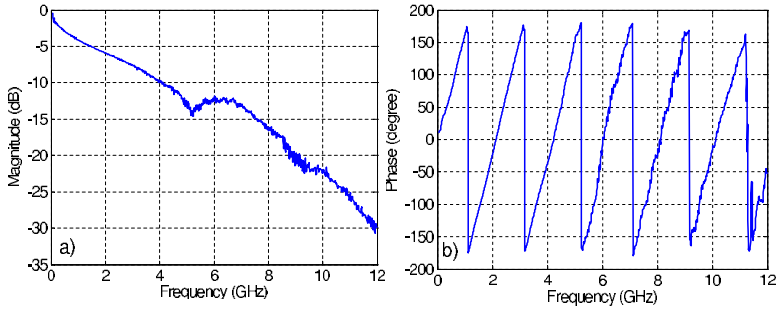

Fig. 3. (a) Magnitude response, and (b) RF Path phase response relative to the Optical Path.

RF Path relative to the Optical Path (ϕ). The magnitude response decreased with increasing frequency. A resonance point at 5.5 GHz is evident which can be attributed to the onset higher order modes. To use this measurements in our experiments, it had been ensured that the cable was completely fixed as the resonance frequency can vary due to vibrations. The phase response is almost linear over the whole band although there are some deviations for frequencies higher than 5.5 GHz. The results of Fig. 3(a) and Fig. 3(b) show that the amplitude and phase of the RF link is well-behaved below 5 GHz, importantly, that the relative phase of the path has an almost linear dependance on frequency in that range. The system will thus be suitable for frequency measurement in this frequency range.

5.2. *Orthogonal Measurements IFM characterization*

The system was configured as depicted in Fig. 2. $\lambda_\circ$, λ_1 and λ_2 were set to 1550, 1551.5, and 1548.5nm respectively. The optical powers corresponding to these three wavelengths were set to 11.7, 17, and 11.7mW respectively. The factor G was calculated to be 0.95, and the delay τ' was 80ps corresponding to nulls in the transversal response at 0 and 12.5 GHz. Both MZMs input impedance (Z_{in}) and photo-detector output impedance (Z_{PD}) were 50Ω. V_π of the both MZMs was 5V. Four different RF power levels ($P_{RF} = 3, 6, 9, 12$ dBm) were used to gain four sets of measurements. Figure 4 shows the measurements taken from digital voltmeters along with the predicted voltage obtained from Eq. (4) and (7). Excellent agreement between predicted and measured results is evident. As the nulls of the transversal filter response (0 and 12.5 GHz)

#95839 - $15.00 USD Received 15 May 2008; revised 14 Aug 2008; accepted 19 Aug 2008; published 21 Aug 2008

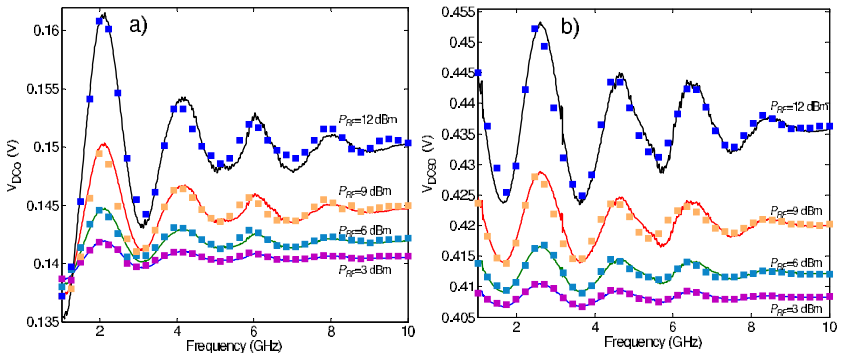

Fig. 4. Measured and predicted results for (a) reference tap and (b) two-tap transversal filter.

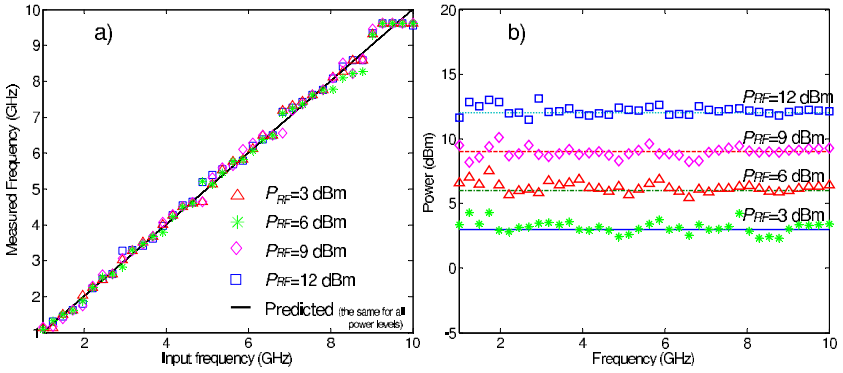

Fig. 5. (a) Measured frequency vs. input frequency. (b) measured and predicted power.

are outside of the frequency measurement range (1-10GHz), they do not severely impact IFM function; however, some fading is evident at the band-edges. These measurements were then used to predict the RF frequency using Eq. (8), and the results are shown in Fig. 5(a). The RF power level was also predicted using Eq. (4) and shown in Fig. 5(b). Good agreement between measurement and prediction results is evident. Due to oscillatory nature of of Eq. (4), and Eq. (7), unambiguous frequency measurement is only possible in each half a period of Fig. 5(a) therefore, there are nine distinct bands within which frequency measurement is unambiguous. Due to zero gradient at peaks and nulls of the sine curve, sensitivity is less at edges of each band. Due to co-axial cable loss at higher frequencies (> 9 GHz), some inconsistencies limit the system functionality. Equation (4) and Eq. (7), indicate a sinusoidal frequency response. By reducing the differential delay τ, the system bandwidth can be increased. Approximating $\phi(\Omega) = \Omega\tau$, it can easily be seen that the sinusoidal period is $\frac{1}{\tau}$ and thus by reducing τ, the sinusoidal period will increase resulting in a wider frequency measurement range. This system shows the ability to measure both RF frequency and power simultaneously.

6. Conclusion

A photonic IFM system has been conceived and practically demonstrated using low cost, low frequency photo-detectors with frequency measurement up to 10 GHz. The system is able to determine RF frequency and power independently and simultaneously. Two orthogonal measurements are obtained employing a broad band RF photonic Hilbert transformer. Wider frequency range can be achieved through integration.

#95839 - $15.00 USD Received 15 May 2008; revised 14 Aug 2008; accepted 19 Aug 2008; published 21 Aug 2008